Acta Oceanol. Sin., 2022, Vol. 41, No. 6, P. 31–40
https://doi.org/10.1007/s13131-021-1907-y
http://www.aosocean.com
E-mail: ocean2@hyxb.org.cn

Distribution and invasion of *Spartina alterniflora* within the Jiaozhou Bay monitored by remote sensing image

Jianbu Wang[1], Zhaoyang Lin[2], Yuanqing Ma[3], Guangbo Ren[1]*, Zijun Xu[4], Xiukai Song[3], Yi Ma[1], Andong Wang[5], Yajie Zhao[5]

[1] Laboratory of Marine Physics and Remote Sensing, First Institute of Oceanography, Ministry of Natural Resources, Qingdao 266061, China

[2] School of Information and Electrics, Beijing Institute of Technology, Beijing 100081, China

[3] Shandong Marine Resources and Environment Research Institute, Shandong Provincial Key Laboratory of Restoration for Marine Ecology, Yantai 264006, China

[4] North China Sea Environmental Monitoring Center, State Oceanic Administration, Qingdao 266033, China

[5] Shandong Yellow River Delta National Nature Reserve Administration Committee, Dongying 257091, China

Received 21 July 2021; accepted 1 September 2021

Abstract

Spartina alterniflora as an alien invasive plant, poses a serious threat to the ecological functions of the coastal wetland of the Jiaozhou Bay. As of 2019, the distribution area of *S. alterniflora* in the Jiaozhou Bay has reached more than 500 hm^2. For this reason, combined with field surveys, remote sensing monitoring of the invasion *S. alterniflora* in the Jiaozhou Bay has been carried out. To accurately identify *S. alterniflora* within the Jiaozhou Bay coastal wetland, we used a new method which is an implement of deep convolutional neural network, and by which we got a higher accuracy than the traditional method. Based on distribution of *S. alterniflora* extracted by the proposed method, the temporal and spatial distribution characteristics of *S. alterniflora* were analyzed. And then combined with environmental factors, the invasion mechanism of *S. alterniflora* in the Jiaozhou Bay was analyzed in detail. From the monitoring results, it can be seen that *S. alterniflora* in Jiaozhou Bay is mainly distributed in the beaches near the Yanghe River Estuary and its southern side, the Dagu River Estuary and the Nügukou. *Spartina alterniflora* first broke out near the Yanghe River Estuary and gradually spread to the tidal flats near the Nügukou. The Dagu River Estuary is dominated by *S. anglica*, whose area has not changed much over the years, and a small amount of *S. alterniflora* has invaded later.

Key words: *Spartina alterniflora*, remote sensing, coastal wetland, deep residual network

Citation: Wang Jianbu, Lin Zhaoyang, Ma Yuanqing, Ren Guangbo, Xu Zijun, Song Xiukai, Ma Yi, Wang Andong, Zhao Yajie. 2022. Distribution and invasion of *Spartina alterniflora* within the Jiaozhou Bay monitored by remote sensing image. Acta Oceanologica Sinica, 41(6): 31–40, doi: 10.1007/s13131-021-1907-y

1 Introduction

Spartina alterniflora is native to North America. However, because of its ability to reproduce asexually and sexually, its strong adaptability and vigorous growth, *S. alterniflora* has been introduced to coastal regions by many countries to protect against erosion by waves and tides (Zuo et al., 2012; Chung, 1993; Maricle and Lee, 2002). The first successful seed germination of *S. alterniflora* in China was carried out in December 1979 (Meng et al., 2020).

Following its introduction, however, the area of *S. alterniflora* has expanded from 260 hm^2 in 1985 to more than 50 000 hm^2 in 2020 in China (Meng et al., 2020). In 2003, *S. alterniflora* was included in the catalog of disastrous invasive species by the State Environment Protection Administration of China and Chinese Academy of Sciences (Wang et al., 2006). Currently, *S. alterniflora* is found in various provinces along the coast. Owing to the strong invasive characteristics of *S. alterniflora*, it gradually occupied tidal flats, replaced local species, and destroyed tidal flat organisms and bird habitats. It has created serious threats to local ecosystems (Brusati and Grosholz, 2007; Callaway and Josselyn, 1992; Daehler and Strong, 1996; Huang and Zhang, 2007; Li and Zhang, 2008). Therefore, there is an urgent need to monitor and analyze the invasion of *S. alterniflora* to provide technical support to prevent and manage the species within the coastal zone.

Field surveys are mainly used to analyze the local ecological environment and the characteristics of *S. alterniflora* after invasion. Because of its wide distribution, fast invasion and the inaccessibility of most coastal wetland areas, field investigations cannot fully capture the invasion characteristics of *S. alterniflora* at a large scale. Remote sensing, however, has the characteristics of large-scale and high frequency coverage, which can monitor *S. alterniflora* invasion patterns quickly and effectively. Historical remote sensing data also allows an analysis of spatiotemporal change in *S. alterniflora* to be carried out (Zuo et al., 2009). Then,

Foundation item: The National Natural Science Foundation of China under contract Nos 42076189, 41206172 and 61601133; the Natural Science Foundation of Beijing under contract No. JQ20021; the Remote Sensing Monitoring Project of Geographical Elements in Shandong Yellow River Delta National Nature Reserve—the Remote Sensing Monitoring Technology Project of *Spartina alterniflora* in Shandong Province in 2020.

*Corresponding author, E-mail: renguangbo@126.com

the invasion mechanism of the species can be analyzed, providing important data support to prevent and control the spread of *S. alterniflora*.

At present, supervised learning based on remote sensing images is still the main method for monitoring invasive species such as *S. alterniflora*. Supervised learning refers to machine learning with available label information. It includes approaches such as maximum likelihood classification (MLC), support vector machine (SVM), random forest (RF), decision trees and artificial neural networks. There are also methods using on-site surveys, such as 3S integration technology. The distribution characteristics of *S. alterniflora* are complex, such as dense distribution with a coverage of 1, sparse distribution with a coverage of less than 0.3, and sparse patches. Its texture characteristics and spectral characteristics are similar to those of reeds, and its distribution area is also affected by tides. These ecological characteristics will bring problems such as mixed pixels, different species with the same spectrum, and different spectra with the same species to remote sensing monitoring. This series of complex issues will bring challenges to the remote sensing monitoring of *S. alterniflora*.

A collective term for remote sensing, geographic information systems (GIS) and global positioning systems (GPS) is 3S technology. Many teams are using 3S technology already to monitor *S. alterniflora*. Tao et al. (2017) used GF-1 satellite remote sensing images and GIS such as ArcGIS and ENVI, combined with GPS to monitor *S. alterniflora* in the intertidal zone of the Guangxi coast. Yao et al. (2017) used 3S to monitor *S. alterniflora* in the Yellow River Delta; Lu and Yang (2018) used the 3S method to visually interpret *S. alterniflora* in the Yellow River Estuary. Sun (2005) combined visual interpretation, MLC and 3S methods to extract information on *S. alterniflora*. Li et al. (2017) used MLC to monitor *S. alterniflora* and mangroves in the Zhangjiang Estuary using data such as Landsat and Google Earth. Zhu et al. (2019) used SVM to visually interpret *S. alterniflora* in the Yellow River Estuary. Tian et al. (2020) used the RF method to extract the information on *S. alterniflora* in the Zhangjiang Estuary, finding it to be better than general MLC. Lin et al. (2015) used decision trees to extract information about *S. alterniflora*. The accuracy rate reached 87% showing that decision trees could extract information on *S. alterniflora* effectively.

Although *S. alterniflora* is distributed in different parts of the coastal zone of China, the invasion characteristics of the species are inconsistent because of different environmental factors, such as tides, and different regional geographical factors (Silinski et al., 2016; Ma et al., 2019; Qin et al., 2009). The Jiaozhou Bay is located in Qingdao City, Shandong Province, China, and the Jiaozhou Bay is a serious area of *S. alterniflora* invasion in China's coastal zone. Understanding how to monitor and analyze the invasion mechanism of *S. alterniflora* in this area using remote sensing has important significance for coastal wetland management, especially in the Jiaozhou Bay. The intertidal zone of the Jiaozhou Bay is a transit station for migratory birds to stop and replenish energy, and it is an important wintering and breeding area for rare waterfowl (Li and Wang, 2013). The Jiaozhou Bay is rich in ecological resources, with a variety of phytoplankton, zooplankton and benthos in the intertidal zone. The invasion by *S. alterniflora* is threatening the local ecosystem. However, there is little research on the invasion of *S. alterniflora* in the Jiaozhou Bay. Existing studies are limited to statistical analysis of the area and spatial distribution, without considering the invasion mechanism of the species.

On the basis of the Landsat and Gaofen-1 WFV multi-spectral remote sensing images, this paper carried out an automatic extraction of *S. alterniflora* over the past 30 years in Jiaozhou Bay using a deep convolutional neural network (DCNN). On the basis of the temporal and spatial distribution of *S. alterniflora*, an analysis of the mechanism of *S. alterniflora* invasion in the Jiaozhou Bay was performed.

The main innovations of this article are as following: (1) A large-scale area of *S. alterniflora* in the Jiaozhou Bay has been investigated on site, combined with remote sensing images to determine the texture and spectral characteristics of *S. alterniflora* in remote sensing images. (2) The remote sensing image has been visually interpreted and deep learning machine interpretation, obtaining the historical distribution of *S. alterniflora* in recent decades. (3) Using the obtained historical distribution, the simple spatial and temporal characteristics of *S. alterniflora* are obtained. The simple reasons and trends of the distribution of *S. alterniflora* in each area are analyzed.

2 Materials and methods

2.1 *Research area*

The Jiaozhou Bay (36°00′–36°20′ N, 120°02′–120°25′ E) is located on the southeast Shandong Peninsula, China, bordering the western Yellow Sea. It is a typical semi-enclosed shallow bay (Fig. 1). In 2016, Qingdao Jiaozhou Bay National Marine Park was established, which is the largest semi-enclosed Bay National Park in China. It is also an import habitat for Asian Pacific migratory birds. At present, more than 300 species of birds have been recorded. The Jiaozhou Bay is fed by a number of rivers, including the Yanghe, Dagu, Meishui, Baisha, Licun and Lianwan rivers. The Jiaozhou Bay has a large area of tidal flat that is rich in biological resources. The typical types of beach vegetation are *Phragmites australis*, *Suaeda salsa*, *S. alterniflo*ra and so on. The area belongs to a temperate monsoon climate, with annual average temperature of 12.2°C and average precipitation of 736.2 mm. There is a regular semidiurnal tide and low tide diurnal inequality. The average sea level in the bay is 2.42 m. The average high tide level

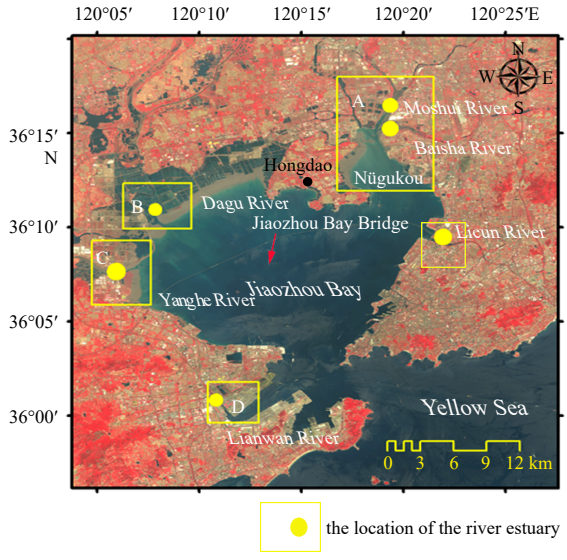

Fig. 1. Study area in the Jiaozhou Bay, Shandong Peninsula, China. Area A is Nügukou, including the Moshui River Estuary, Baisha River Estuary and tidal flat on the east side of Hongdao; Area B is the Dagu River Estuary; Area C is the Yanghe River Estuary; and Area D is the Lianwan River Estuary.

is 3.81 m and the average low tide level is 1.02 m (Li and Wang, 2013).

2.2 *Remote sensing data*

In this paper, medium resolution satellite images with a long time series were used to monitor *S. alterniflora* in the Jiaozhou Bay, including Landsat 5 TM, Landsat 7 ETM+, Landsat 8 OLI series images and Gaofen-1 WFV (Table 1), Landsat data download platforms are the official website of the US Geological Survey (https://landsatlook.usgs.gov/viewer.html) and the official website of Geospatial Data Cloud (http://www.gscloud.cn/). To identify *S. alterniflora* accurately, the images were captured between August and October, which is the most vigorous growth time of the species and is the time when the spectral characteristics of the image are most obvious (Ren et al., 2019). The acquired remote sensing data has been subjected to atmospheric correction, radiation correction and orthorectification.

2.3 *Field survey data*

We conducted field surveys of *S. alterniflora* in the Jiaozhou Bay in 2017, 2018 and 2019. We obtained a total of 50 sites through handheld GPS (precise positioning), of which 30 sites were in the same location for three years, 12 sites were added in 2018, and 16 sites were added in 2019. Each picture was on both having latitude and longitude. Combining the texture features, spectral features and boundary information of *S. alterniflora* in different remote sensing images, the sample information for remote sensing classification and accuracy verification was established. The field survey is shown in Fig. 2.

Table 1. Details of satellite images used in this analysis

Image name	Imaging time	Space resolution/m
Landsat 5 TM	1988–2008	30
Landsat 7 ETM+	2012–2014	30
Landsat 8 OLI	2015–2019	15
Gaofen-1 WFV	2014–2019	16

The vegetation in the Jiaozhou Bay mainly includes *S. alterniflora*, *P. australis*, *Suaeda salsa* and a few *S. anglica*. Because the area of *S. anglica* is much smaller than the area of *S. alterniflora* and in some areas the two species co-occur, we classified *S. anglica* and *S. alterniflora* into the same category and did not attempt to extract them separately (Fig. 2). Figure 2 shows the distribution of survey sites and field survey areas in the Jiaozhou Bay, and the different environments of *S. alterniflora* distribution. According to the field investigation, *S. alterniflora* was mainly distributed in the vicinity of the Nügukou, Dagu River Estuary and Yanghe River Estuary, with a small area of *S. anglica* in the Lianwan River Estuary. Next, remote sensing visual interpretation is performed to obtain the ground truth of *S. alterniflora* in 2017, 2018 and 2019. For a spatial resolution of 15 m, the number of *S. alterniflora* pixels in 2017 was 16 449, the number of *S. alterniflora* pixels in 2018 was 21 368, and the number of *S. alterniflora* pixels in 2019 was 25 698. These data are used for the following algorithm verification and prediction of the distribution of *S. alterniflora* in other years.

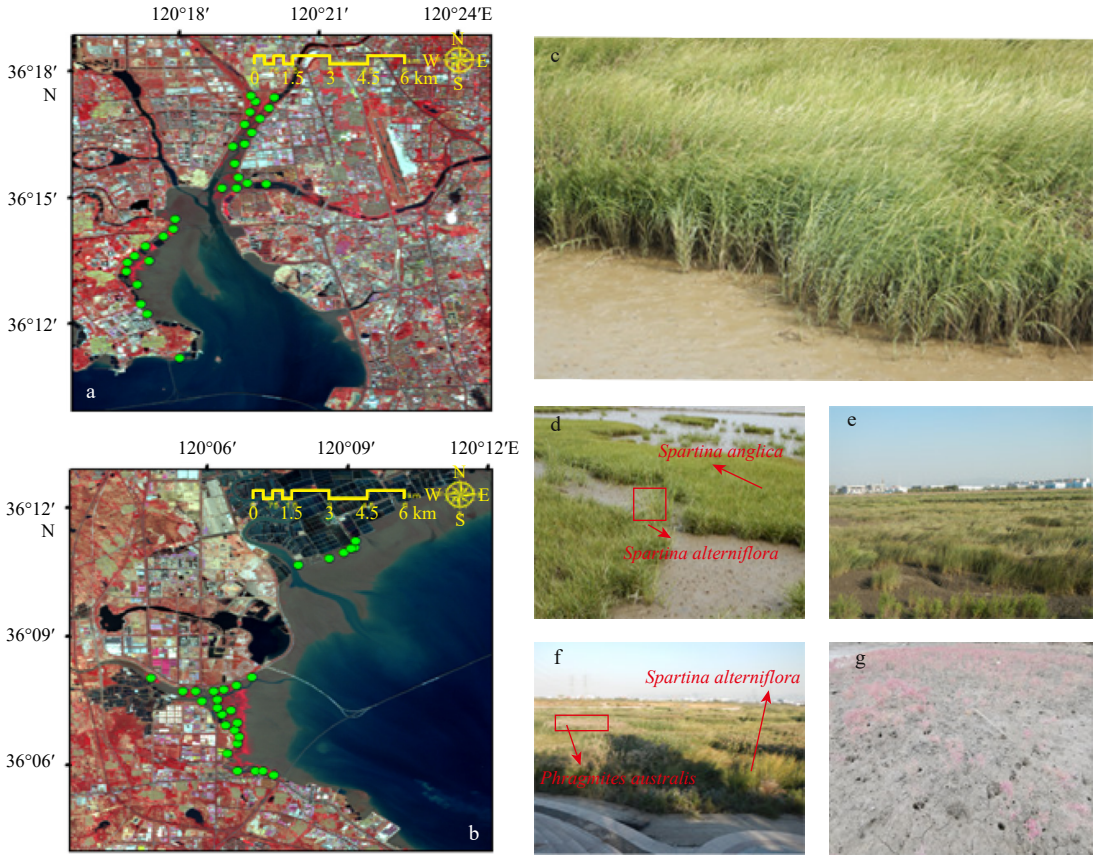

Fig. 2. Field survey sites (a, b; green dots) and vegetation photographs (c–g). c. Dense growth of *Spartina alterniflora* on the tidal flat; d. *S. anglica* mixed with *S. alterniflora*, which is mainly distributed in the Dagu River Estuary; e. densely distributed *S. alterniflora* blocking the river channel; f. *S. alterniflora* occupying the growing area of *Phragmites australis*; g. *Suaeda salsa* near *S. alterniflora*, mainly in the Yanghe River Estuary and the Moshui River Estuary.

2.4 *Methods*

To extract *S. alterniflora* information from remote sensing images, we regarded *S. alterniflora* as one category and the rest of the environment as another category. Here, a solution is proposed using the vegetation indexes and the deep residual network.

A vegetation index (VI) is a radiation value that reflects the relative abundance and activity of green vegetation. They are often used to describe the physiological conditions of vegetation, and to estimate variables such as the area of different land covers, plant photosynthetic capacity, leaf area index, existing green biomass and vegetation productivity. More than one hundred vegetation indices have been proposed. The most commonly used ones include the normalized difference vegetation index (NDVI) (Tucker, 1979), ratio vegetation index (RVI) (Pearson and Miller, 1972), differential vegetation index (Qi et al., 1994), perpendicular vegetation index (Richardson and Weigand, 1977), soil-adjusted vegetation index (Jordan, 1969) and modified soil-adjusted vegetation index (MSAVI) (Huete, 1988).

$$\mathrm{NDVI} = \frac{\rho_{\mathrm{NIR}} - \rho_{\mathrm{RED}}}{\rho_{\mathrm{NIR}} + \rho_{\mathrm{RED}}}, \tag{1}$$

$$\mathrm{RVI} = \frac{\rho_{\mathrm{NIR}}}{\rho_{\mathrm{RED}}}, \tag{2}$$

$$\mathrm{MSAVI} = \frac{\rho_{\mathrm{NIR}} + 0.5 - \sqrt{(2\rho_{\mathrm{NIR}} + 1)^2 - 8(\rho_{\mathrm{NIR}} - \rho_{\mathrm{RED}})}}{2}. \tag{3}$$

In this paper, three vegetation indices: NDVI, RVI and MSAVI are utilized. Eqs (1), (2) and (3) represent NDVI, RVI and MSAVI, respectively. Among these, ρ is the reflectivity, NIR is the near infrared band and RED is the red band of the visible light. After linking these three vegetation indices to Gaofen-1 WFV, we obtained an image with seven channels. We used the processed data and the original data. The data processing flow is shown in Fig. 3.

2.4.1 *DCNN*

A convolutional neural network (CNN) is a feedforward deep network that uses convolution operations. It is one of the representative algorithms of deep learning and has broad applications in pattern recognition and target detection. Multispectral images (MSI) capture spectral information across multiple wave lengths, and they are often processed using CNN techniques.

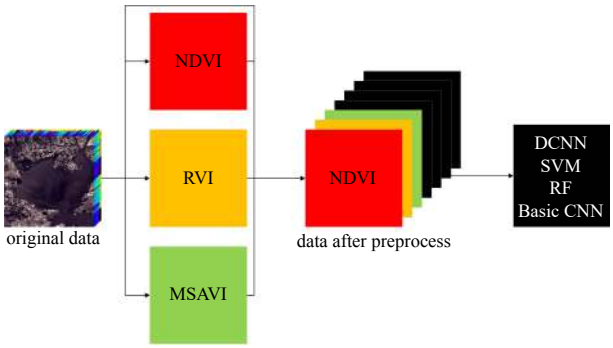

Fig. 3. Data preparation and experimental process. NDVI is the abbreviation of the normalized difference vegetation index; RVI, the ratio vegetation index; MSAVI, the modified soil-adjusted vegetation index; CNN, the convolutional neural network; DCNN, deep convolutional neural network; SVM, the support vector machine; RF, random forest.

For traditional remote sensing CNN, they only use a few convolutional layers and pooling layers. This is obviously not enough. In the field of computer vision, the improvement brought by DCNNs cannot be underestimated. However, simply increasing the number of CNN layers does not always improve its performance. With the increase of the number of layers, the performance of the network is usually first improved within a certain range and then decreased, which is mainly due to the vanishing gradient and overfitting. Vanishing gradient means that as the number of layers increases, the gradient of the network's backpropagation gradually becomes 0. Overfitting means that in the training process, because the training data contains sampling errors, the complex model will also take the sampling error into consideration. Inside, the sampling error is also well fitted. Fortunately, the residual connection, which directly connects the front and back of the network, can effectively reduce the adverse effects of the above problems. Based on the above ideas, a DCNN including cascade block (Li et al., 2018) was proposed to extract the distribution of *S. alterniflora* in MSIs. As pointed out in Fig. 4, the two orange addition operations are the concrete manifestation of the residual connection in the proposed DCNN.

The cascade block is shown in the red box in Fig. 4. A cascade block consists of two additive residual connections, five 2-D convolutional layers, two LeakyReLU layers and one Batch Normalization (BN) layer. For the overall proposed DCNN, as shown in Fig. 4, it consists of many effective layers. In Fig. 4, LeakyReLU is a nonlinear activation function that introduces nonlinear factors into the network. The role of the BN layer and the Dropout layer is to reduce overfitting. The function of the Maxpooling layer is to reduce the image size and the computational complexity. The goal of the Flatten layer is to convert a multi-dimensional vector to a 1-D vector and the fully connected output layer uses the Sofmax activation function to achieve the predicted probability output of the network.

2.4.2 *Other comparison methods*

The DCNN is compared with three other approaches. SVM (Hsu et al., 2003) is a binary classification model, which combines a linear classifier with the largest interval defined in the feature space and kernel techniques that are non-linear. The learning strategy of SVM is to maximize the interval and to minimize the regularized hinge loss function, which can be formalized as a convex quadratic programming problem. Thus, the learning algorithm of SVM is the optimal algorithm for solving convex quadratic programming. The RF (Breiman, 2001) algorithm integrates multiple trees through ensemble learning. Its basic unit is a decision tree, and it belongs to a large branch of machine learning. A decision tree divides information into two sections at a node based on the maximum difference between the two groups. Multiple trees use subsets of data and average the results. The concept of a forest, containing multiple trees, is the main idea behind random forest-integrated thinking. A basic CNN is also utilized for comparison experiments. It contained two convolutional layers: a Maxpooling layer and a fully connected layer. The output layer used the Softmax layer.

2.5 *Experiments*

Three experiments are conducted. The first group experimented with the original GF-1 WFV and vegetation indices. The second group used only GF-1 WFV. Both sets of experiments tested the four methods. The last group uses only DCNN to clas-

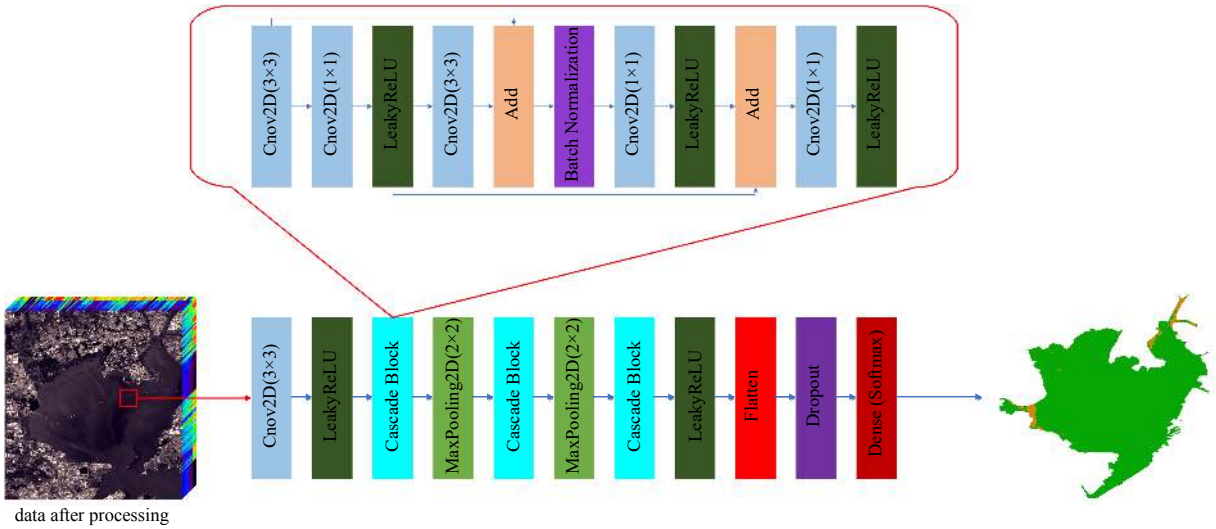

Fig. 4. Network structure of the deep convolutional neural network.

sify data sets of different years and satellite images. For the data set of each year, we first use the coastline obtained through the field survey to remove the land above the coastline from the data set. This is because *S. alterniflora* is a salt water plant, and it cannot grow on dry land. For each year used for verification, depending on the number of samples, 0.5% surrounding samples and 20% *S. alterniflora* samples are selected as the training set. The test set is the samples determined by the field survey to comprehensively evaluate the performance of the classifier. It should be noted that only the distribution of *S. alterniflora* in 2017, 2018 and 2019 is the result of field investigation. They can be used to verify the effectiveness of the algorithm, and the distributions in other years are the results of using the model to judge.

Because it is a binary classification experiment, recall, precision and F1-score are added to the overall accuracy (OA). The precision indicates how many of the samples whose predictions are positive are correct. The recall is how many positive samples are predicted correctly. F1-score refers to the harmonic mean of precision and recall, which can more comprehensively evaluate the performance of the classifier. For binary classification tasks with very unbalanced samples, it is more appropriate to use F1-score as the evaluation criterion. *S. alterniflora* is identified as the positive sample.

3 Results

3.1 *Classification results and analysis*

Table 2 shows the results for the first two groups of experiments. The OA of the four methods was very high, over 97%. However, the recall rate of SVM was very low, only 29.55% and 29.53%. Because this task is a distributed extraction task, there are far more surrounding samples than target samples. The reason for the very low recall is mainly that the classifier roughly divides most samples into surrounding samples for high OA. When evaluating a classifier, recall and precision must be considered comprehensively. So F1-score is the best evaluation index for this task. Although the precision of SVM is the highest among all methods, its F1-score is still the worst. Furthermore, it can be concluded that for this task, the performance of SVM is the worst.

We also found that when the vegetation indices were not used, the CNN results were better than those of the DCNN. This was caused by overfitting. Although DCNN had a deeper and more complex network, the model capacity was greater. This required more training data to arrive at the most appropriate weights. If there were no vegetation indices, there were only four channels of data and the corresponding data complexity decreased. That caused more complicated DCNN overfitting.

The amount of data in this experiment was relatively large. For complex data, the performance of RF is not ideal. It can be seen from Table 2 that adding or not adding vegetation indices had little effect on RF. Although the various indicators of RF were stable, Table 2 shows that all indicators were weaker than the DCNN using vegetation indices. The vegetation indices had the greatest impact on our proposed DCNN. Its F1-score increased from 0.513 3 to 0.748 5. It can be seen that for this experiment, the

Table 2. GF-1 data classification results (%) of the Jiaozhou Bay in 2019

Method	*Spartina altemiflora*	Surrounding	OA	Recall	Precision	F1-score
DCNN	98.75	98.97	98.97	98.75	60.27	74.85
SVM	29.55	99.99	98.90	29.55	98.30	45.44
RF	98.55	98.44	98.39	95.63	49.21	64.99
Basic CNN	98.55	98.44	98.33	98.55	48.17	64.71
DCNN (no)	99.12	97.04	97.08	99.12	34.63	51.33
SVM (no)	29.53	99.99	98.90	29.53	98.30	45.42
RF (no)	95.57	98.51	98.46	95.57	50.28	66.57
Basic CNN (no)	98.29	98.29	98.29	98.29	47.65	64.18

Note: OA is the abbreviation of the overall accuracy; DCNN, deep convolutional neural network; SVM, the support vector machine; RF, the random forest; CNN, the convolutional neural network. “no” in bracket means that the vegetation index is not used.

addition of the vegetation indices satisfied the data complexity of DCNN. All in all, DCNN achieves the highest F1-score and OA compared to other methods, which shows that the performance of DCNN with vegetation index is significantly better than other comparison methods from two different dimensions.

As shown in Table 3, for the generalization ability of the proposed DCNN, four experiments were performed on different satellite images in different years. Since most of the original Landsat8 and Landsat7 bands only have a spatial resolution of 30 m, the spatial resolution of all bands of GF-1 is 16 m. The Landsat8 data in 2017 is uniformly upsampled to 15 m to make the experiment fair. The classification result of R8 in 2017 is much better than that of L8, which is due to the increase in sample size and the reduction of possible mixed pixels after upsampling. The difference between GF-1 and R8 in 2019 is mainly caused by information redundancy and inaccuracy brought about by upsampling. But the gap is not big. The difference between L7 and L8 in 2017 is very small, which shows that the proposed method can be applied to both L7 and L8. In general, the proposed DCNN can be performed on different satellite images and in different years.

Figures 5a–c shows the distribution results of *S. alterniflora* in several typical years in the Jiaozhou Bay based on the new method that we proposed.

3.2 *Temporal distribution characteristics of S. alterniflora*

Since 1988, *S. alterniflora* has been monitored every 5–8 years in Jiaozhou Bay, as shown in Fig. 6. It was found that the area of *S. alterniflora* showed no significant change before 2014 and covered less than 60 hm^2. However, after 2014, the area rapidly increased and reached 588.6 hm^2 by 2019. To analyze the reasons for the explosive growth of *S. alterniflora* after 2014, the monitoring frequency was increased. The blue histograms in Fig. 6 show the annual monitoring results of *S. alterniflora* from 2012 to 2019. From the monitoring results, the annual increase of *S. alterniflora* from 2013 to 2019 was 88.9 hm^2, and the annual increment was larger than the whole area of *S. alterniflora* in 2013, which was 55.1 hm^2.

According to the spatial distribution characteristics of *S. alterniflora* in the Jiaozhou Bay, the species was mainly distributed

Table 3. Classification results (%) of the Jiaozhou Bay images from different satellites in different years

Method	*Spartina altemiflora*	Surrounding	OA	Recall	Precision	F1-score
DCNN (R8 2017)	98.12	98.90	98.83	98.12	47.08	63.63
DCNN (L8 2017)	95.24	97.93	97.91	95.24	25.04	39.65
DCNN (L7 2017)	88.24	98.27	98.20	88.24	27.01	41.36

Note: OA is the abbreviation of the overall accuracy; DCNN, deep convolutional neural network. R8 refers to the image upsampled by Landsat 8 to a spatial resolution of 15 m. L8 and L7 refer to Landsat 8 and Landsat 7, respectively.

Fig. 5. Remote sensing monitoring results of *Spartina alterniflora* over time in the Jiaozhou Bay. a. *Spartina alterniflora* distribution in the Yanghe River Estuary and Dagu River Estuary in 2002, 2012, 2014 and 2019; b. *S. alterniflora* distribution in Nügukou in 2013, 2015, 2017 and 2019; c. *S. alterniflora* distribution in the Lianwan River Estuary in 1988, 2013, 2015 and 2019.

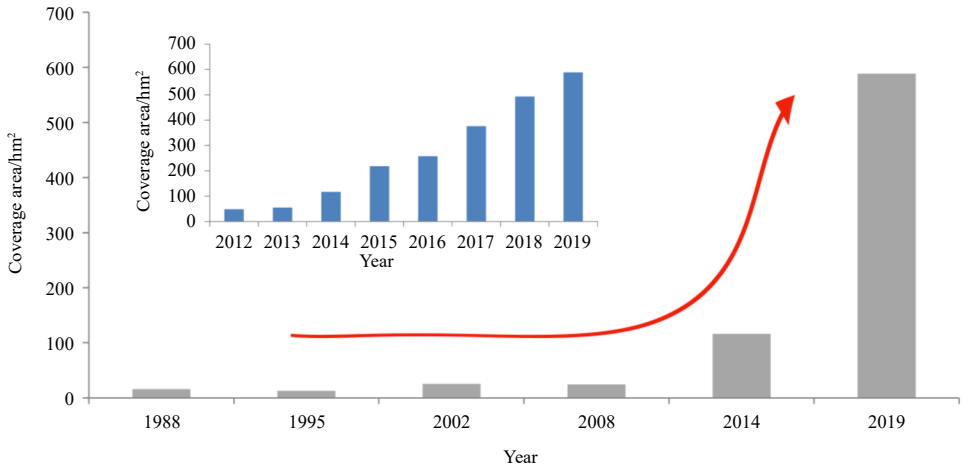

Fig. 6. Bar chart of changes in the area of *Spartina alterniflora* in the Jiaozhou Bay, 1988–2019. The gray color shows intermittent monitoring before 2019. The blue color shows annual monitoring after 2012.

in four areas: Nügukou, Yanghe River Estuary, Dagu River Estuary and Lianwan River Estuary. As shown in Fig. 7, the area of *S. alterniflora* near the Yanghe River Estuary changed little from 1988 to 2008 and was less than 10 hm². It began to expand rapidly in 2012 and 2013, and the area reached more than 30 hm². The area of *S. alterniflora* in Yanghe River Estuary continued to increase sharply, reaching 99.2 hm² in 2014 and 297.8 hm² in 2019.

The area of *S. alterniflora* near Nügukou did not change much before 2014, covering less than 10 hm². However, it increased rapidly after that, reaching 86.5 hm² in 2015 and 277.8 hm² in 2019. The Dagu River Estuary contained *S. anglica* with small area of *S. alterniflora*, and Lianwan River Estuary mostly contained *S. anglica*. The area of occurrence in the Dagu River Estuary has changed little since 1988, remaining at less than 14 hm². The area of *S. anglica* in the Lianwan River Estuary decreased gradually after 2008 and, at its largest, was no more than 8 hm².

3.3 *Spatial distribution characteristics of S. alterniflora*

According to the distribution characteristics of *S. alterniflora* over time, the species was first found in the south side of the Yanghe River Estuary near the western end of Jiaozhou Bay Bridge. It was a small area of only 5.0 hm², which increased to 32.3 hm² in 2012. The patches of *S. alterniflora* were relatively scattered. After 2014, the number of patches on the south side of the estuary grew rapidly. By 2019, the patches of *S. alterniflora* had amalgamated and began to invade the river. According to the distribution results of *S. alterniflora* in the Jiaozhou Bay in 2019, the largest patch area was in the Yanghe River Estuary, especially from the river mouth to the Jiaozhou Bay Bridge. This patch was 4.4 km long and the maximum width was 2.4 km (Fig. 5a).

Before 2014, the *S. alterniflora* in Nügukou was found in the mouth of the Baisha River Estuary with an area of less than 5.0 hm². It did not greatly change for many years. However, since 2015, the area has rapidly grown, mainly in the river channel of the Moshui River Estuary and on the east beach of Hongdao (Fig. 5b). In the Baisha River Estuary, the area has slightly increased. By 2019, the river channel of the Nügukou and the Moshui River Estuary had been invaded and almost blocked by *S. alterniflora*. The maximum length of the S. *alterniflora* patches was 5.1 km. In the Hong-

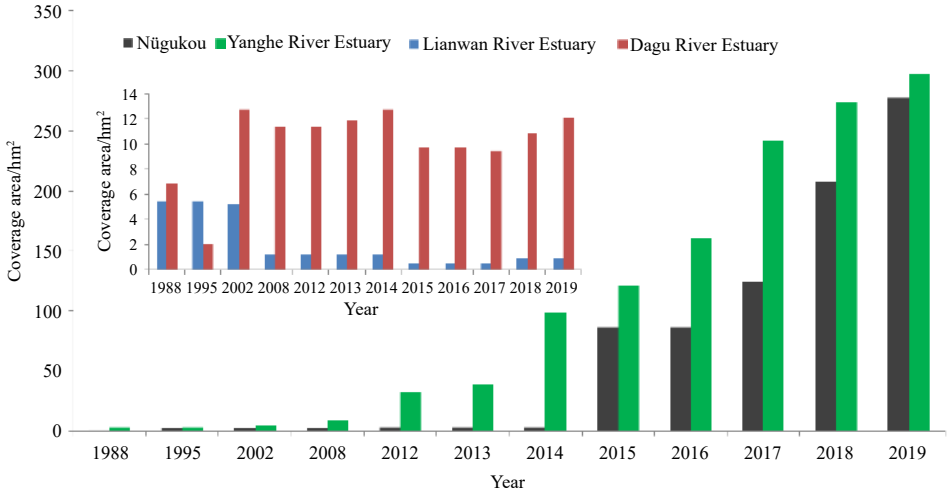

Fig. 7. Bar chart of *Spartina alterniflora* area in different distribution areas in the Jiaozhou Bay. Green shows the area of *S. alterniflora* each year in the Yanghe River Estuary; black shows the area of *S. alterniflora* near Nügukou; blue and red represent the area of *S. alterniflora and S. anglica* in the Dagu River Estuary and Lianwan River Estuary, respectively.

dao area, except for the aquaculture ponds, the surrounding beaches were mostly occupied by *S. alterniflora*. The maximum width of the patches was 0.8 km from land to sea.

The distribution area of *S. alterniflora and S. anglica* in the Dagu River Estuary was relatively small. The distribution patches are relatively fragmented and are mainly distributed in the northeast of the Dagu River Estuary without obvious change for many years (Fig. 5a).

In 1988, *S. anglica* was mainly distributed in the south of the Lianwan River Estuary mouth. With the reclamation, the area of *S. anglica* reduced from 5.5 hm^2 in 1988 to 0.9 hm^2 in 2019.

4 Discussion

Owing to different environmental factors, the invasion characteristics of *S. alterniflora* vary in different regions. In this study we examined the invasion of *S. alterniflora* in the Jiaozhou Bay.

4.1 *Invasion of S. alterniflora in the Yanghe River Estuary*

As a kind of invasive vegetation, several factors are favorable for its expansion, that are the minimal impact of tidal currents, adequate available nutrients to sustain both germination and plant growth, the soft sediment facilitating rapid rooting and fixation of seedlings (Ren et al., 2019), and fresh water for seed to germinate (Qin et al., 1985). With the construction of the Jiaozhou Bay Bridge, the hydrodynamic flow has been changed, particularly the area close to the pier, the tidal flow has been weakened (Shi et al., 2018) and the weakened tidal flow around the bridge has promoted sedimentation, created favorable conditions, for the fixation of the seedings and the rapid rooting. So the initial invasion was from the seeds of *S. alterniflora* and in the second and subsequent years, both root and seed propagation methods occurred to rapidly increase the patch size (Davis and Thompson, 2000; Huang and Zhang, 2007). In 2012 and 2013, one year after the completion of the bridge in 2011, the area of *S. alterniflora* began to increase and a large area of *S. alterniflora* was formed in 2014. This outbreak was basically consistent with the construction of the bridge.

The relationship between the expansion and invasion of *S. alterniflora* and the Jiaozhou Bay Bridge is given above. Now we analyze the invasion process of *S. alterniflora.* The construction of the bridge weakened the hydrodynamic force around the north side of the bridge (Shi et al., 2018). This led to sediment deposition on the north side of the bridge and formed a beach conducive to the invasion of *S. alterniflora* seeds (Ren, 2019). As it spreads, *S. alterniflora* itself also promotes siltation. It formed a favorable environment for seed germination on the open beach at the mouth of the river with more fresh water and rich nutrition, which accelerated the spread of *S. alterniflora.* This explains why large-scale outbreaks of *S. alterniflora* began to appear at the mouth of the Yanghe River in 2014 after a two-year increase in the estuary, and by 2019 almost occupied the beach and river channel. This pattern shows that there is a correlation between the Jiaozhou Bay Bridge and the invasion process of *S. alterniflora* in space.

Figure 8 shows the Gaofen-1 WFV image near the western end of Jiaozhou Bay Bridge in 2019. The southernmost end of the distribution area of *S. alterniflora* is inside the Bay on the north side of the bridge (A). At the point B on the seaward side of the bridge (south side), there is no vegetation growing on the beach. Because of the construction of the bridge, the hydrodynamic force inside of the bridge is weakened and sedimentation is promoted, which is conducive to the invasion of *S. alterniflora.* Therefore, we consider that the construction of Jiaozhou Bay Bridge is consistent with the invasion of *S. alterniflora* in time and space.

4.2 *Invasion of S. alterniflora in Nügukou*

From the analysis shown above, we found that the main expansion of *S. alterniflora* in Nügukou was in 2015, one year later than in the Yanghe River Estuary. This is probably because *S. alterniflora* first broke out in the Yanghe River Estuary and produced a large number of seeds which were transported to Nügukou by tidal flows and currents. Furthermore, *S. alterniflora*'s germination rate in freshwater as high as 90% ,which is

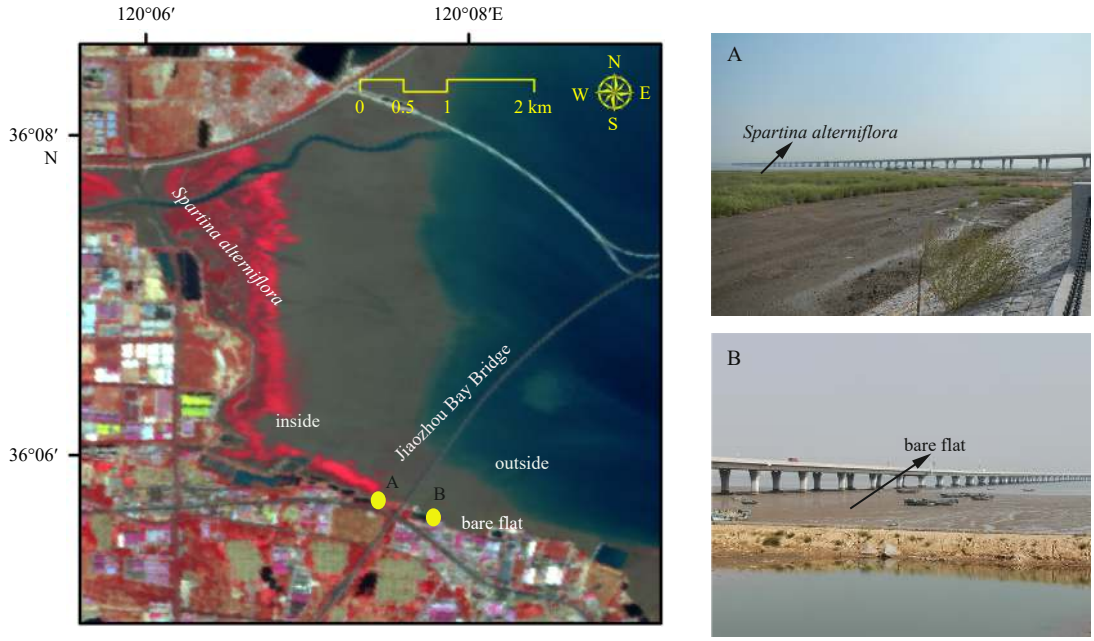

Fig. 8. *Spartina alterniflora* distribution from the Gaofen-1 WFV image and field pictures near the western end of Jiaozhou Bay Bridge. The red features in the image are *S. alterniflora.* The site conditions of the beach at A and B are shown on the right.

higher than in seawater (Qin et al., 1985). In Nügukou, many estuaries such as the Moshui River and Baisha River provide fresh water and rich nutrition to Nügukou, which is conducive to seed germination. After that, on the basis of reproduction from roots and seeds, *S. alterniflora* rapidly expanded, occupying tidal flats and river channels (Fig. 9).

4.3 *Invasion of S. alterniflora in the Dagu River Estuary and Lianwan River Estuary*

Owing to the large-scale reclamation around the Dagu River Estuary, the tidal flats are in a state of erosion (Fan, 2005) which is not conducive to seed burial and germination and inhibits the invasion of *S. alterniflora*. The area of *S. alterniflora* is small and scattered and has not changed much over the years (Figs 5a and 7). *Spartina alterniflora* can invade through seeds only in *S. anglica* distribution areas because of the presence of silt (Fig. 10).

In the Lianwan River Estuary, *S. anglica* has been artificially introduced to a small area. It is affected by reclamation and the area is generally decreasing (Figs 5c and 7).

4.4 *Invasion of S. alterniflora in other areas of the Jiaozhou Bay*

There is a large area of tidal flats between the Dagu River Estuary and Nügukou. However, this area is similar to the Dagu River Estuary with a large area of reclamation, which erodes the tidal flats. This area lacks the two factors of siltation and fresh water which required for the invasion of *S. alterniflora*. In other areas of the Jiaozhou Bay, the construction of ports, wharfs and dams have also reduced sedimentation. Therefore, *S. alterniflora* is not present in these areas.

5 Conclusions

On the basis of the remote sensing data for *S. alterniflora* in the Jiaozhou Bay over the past 30 years, this study created accurate spatial and temporal distribution information on *S. alterniflora* in the Jiaozhou Bay using the new DCNN method. We found that *S. alterniflora* was mainly distributed in the Yanghe River Estuary, Dagu River Estuary and Nügukou. The Lianwan River Estuary also has a small area of the species. *Spartina alterniflora* in the Jiaozhou Bay increased from 16.1 hm^2 in 1988 to 588.6 hm^2 in 2019, which is an increase of 36.5 times. A large-scale period of explosive growth began around 2014, first in the Yanghe River Estuary and then in Nügukou in 2015. By combining the hydrodynamic influence of Jiaozhou Bay Bridge and the comparative analysis of *S. alterniflora* invasion characteristics, we found that the construction of the bridge is one of the key reasons for the large-scale outbreak of *S. alterniflora*.

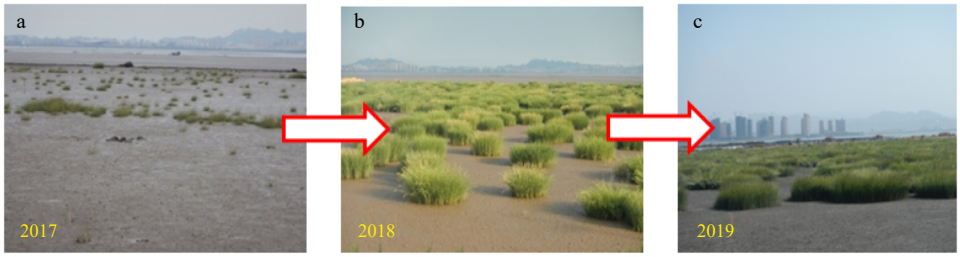

Fig. 9. Invasion process of *Spartina alterniflora* on the east tidal flat of Hongdao. a. The invasion of *S. alterniflora* through seed. The initial stage shows scattered *S. alterniflora* seedlings. b. *Spartina alterniflora* starts root propagation after the seed invasion and forms a large number of patches. The patches are almost circular and spaced apart from each other. c. *Spartina alterniflora* multiplies through seeds and roots to connect the patches and finally completes the occupation of the tidal flat.

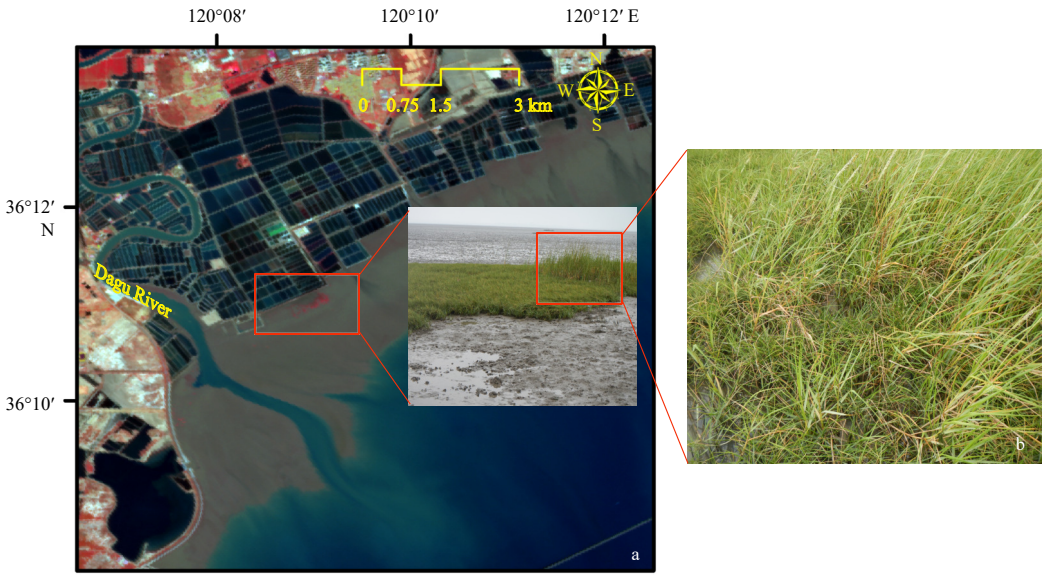

Fig. 10. Scattered *Spartina anglica* at the Dagu River Estuary and *S. alterniflora* invading in the *S. anglica* growing area. a. The Gaofen-1 WFV satellite image and the photographs of *S. anglica* invaded by *S. alterniflora*; b. a mixed area of *S. anglica* and *S. alterniflora* taken at the scene. The taller plants are *S. alterniflora*, the smaller plants are *S. anglica*.

Acknowledgements

The authors would like to thank the USGS for providing satellite images.

References

Breiman L. 2001. Random forests. Machine Learning, 45(1): 5–32, doi: 10.1023/A:1010933404324

Brusati E D, Grosholz E D. 2007. Effect of native and invasive cordgrass on *Macoma petalum* density, growth, and isotopic signatures. Estuarine, Coastal and Shelf Science, 71(3–4): 517–522

Callaway J C, Josselyn M N. 1992. The introduction and spread of smooth cordgrass (*Spartina alterniflora*) in South San Francisco Bay. Estuaries, 15(2): 218–226, doi: 10.2307/1352695

Chung C H. 1993. Thirty years of ecological engineering with *Spartina* plantations in China. Ecological Engineering, 2(3): 261–289, doi: 10.1016/0925-8574(93)90019-C

Daehler C C, Strong D R. 1996. Status, prediction and prevention of introduced cordgrass *Spartina* spp. invasions in Pacific estuaries, USA. Biological Conservation, 78(1–2): 51–58, doi: 10.1016/0006-3207(96)00017-1

Davis M A, Thompson K. 2000. Eight ways to be a Colonizer; two ways to be an invader: a proposed nomenclature scheme for invasion ecology. Bulletin of the Ecological Society of America, 81(3): 226–230

Fan Jianyong. 2005. Monitoring dynamic changes of coastline around Qingdao and its adjacent coastal zone using remote sensing (in Chinese)[dissertation]. Qingdao: The Institute of Oceanology, Chinese Academy of Sciences

Hsu Chih-Wei, Chang Chih-Chung, Lin Chih-Jen. 2003. A practical guide to support vector classification. Taiwan, China: Department of Computer Science and Information Engineering, National Taiwan University

Huang Huamei, Zhang Liquan. 2007. A study of the population dynamics of *Spartina alterniflora* at Jiuduansha shoals, Shanghai, China. Ecological Engineering, 29(2): 164–172, doi: 10.1016/j.ecoleng.2006.06.005

Huete A R. 1988. A soil-adjusted vegetation index (SAVI). Remote Sensing of Environment, 25(3): 295–309, doi: 10.1016/0034-4257(88)90106-X

Jordan C F. 1969. Derivation of leaf-area index from quality of light on the forest floor. Ecology, 50(4): 663–666, doi: 10.2307/1936256

Li Yi, Chen Yining, Li Yan. 2017. Remote sensing analysis of the changes in the ecotone of mangrove forests and *Spartina alterniflora* saltmarshes. Marine Science Bulletin, 36(3): 348–360

Li Xiang, Li Wei, Xu Xiaodong, et al. 2018. CascadeNet: modified resnet with cascade blocks. In: 2018 24th International Conference on Pattern Recognition. Beijing: IEEE, 483–488

Li Jingmei, Wang Xiaoling. 2013. Wetland reclamation and habitat damage assessment in Jiaozhou Bay. Resources Science, 35(1): 59–65

Li Hepeng, Zhang Liquan. 2008. An experimental study on physical controls of an exotic plant *Spartina alterniflora* in Shanghai, China. Ecological Engineering, 32(1): 11–21, doi: 10.1016/j.ecoleng.2007.08.005

Lin Wenpeng, Chen Guangsheng, Guo Pupu, et al. 2015. Remote-sensed monitoring of dominant plant species distribution and dynamics at Jiuduansha wetland in Shanghai, China. Remote Sensing, 2015, 7(8): 10227–10241

Lu Feng, Yang Junfang. 2018. Remote sensing monitoring and analysis of *Spartina alterniflora* based on Landsat 8 OLI satellite data—taken the Shandong Yellow River Delta National Nature Reserve as an example. Shandong Forestry Science and Technology, 48(1): 29–32

Ma Xu, Yan Jiaguo, Wang Fangfang, et al. 2019. Trait and density responses of *Spartina alterniflora* to inundation in the Yellow River Delta, China. Marine Pollution Bulletin, 146: 857–864, doi: 10.1016/j.marpolbul.2019.07.022

Maricle B R, Lee R W. 2002. Aerenchyma development and oxygen transport in the estuarine cordgrasses *Spartina alterniflora* and *S. anglica*. Aquatic Botany, 74(2): 109–120, doi: 10.1016/S0304-3770(02)00051-7

Meng Weiqing, Feagin R A, Innocenti R A, et al. 2020. Invasion and ecological effects of exotic smooth cordgrass *Spartina alterniflora* in China. Ecological Engineering, 143: 105670, doi: 10.1016/j.ecoleng.2019.105670

Pearson R L, Miller L D. 1972. Remote mapping of standing crop biomass for estimation of the productivity of the short-grass prairie. In: Proceedings of the Eighth International Symposium on Remote Sensing of Environment. Ann Arbor: ERIM International, 1357–1381

Qi J, Chehbouni A, Huete A R, et al. 1994. A modified soil adjusted vegetation index. Remote Sensing of Environment, 48(2): 119–126, doi: 10.1016/0034-4257(94)90134-1

Qin Yingying, Jiang Xiaoxiao, Li Feng, et al. 2009. Morphological plasticity and biomass allocation of *Spartina alterniflora* lossel in different habitats. Marine Environmental Science, 28(6): 657–659, 667

Qin Pei, Jing Meide, Xie Min. 1985. The comparison of three ecotypes of Sparina alterniflora in coastal marshes of Luoyuanwan, Fujian Province. Journal of Nanjing University: Natural Science, 40: 226–236

Ren Guangbo, Wang Jinjin, Wang Andong, et al. 2019. Monitoring the invasion of smooth cordgrass *Spartina alterniflora* within the modern Yellow River Delta using remote sensing. Journal of Coastal Research, 90(S1): 135–145

Richardson A J, Weigand C L. 1977. Distinguishing vegetation from soil background information. Photogrammetric Engineering and Remote Sensing, 43(12): 1541–1542

Shi Xiaoyu, Zhang Ridong, Zhang Wenjing, et al. 2018. Impact of Jiaozhou Bay cross-sea bridge on winter ice formation in northern Jiaozhou Bay. Marine Science Bulletin, 37(6): 633–642

Silinski A, Van Belzen J, Fransen E, et al. 2016. Quantifying critical conditions for seaward expansion of tidal marshes: a transplantation experiment. Estuarine, Coastal and Shelf Science, 169: 227–237

Sun Samei. 2005. Monitoring of smooth cordgrass invasion by remote sensing in Sandu Bay, Fujian. Journal of Oceanography in Taiwan Strait, 24(2): 223–227

Tao Yancheng, Pan Lianghao, Fan Hangqing, et al. 2017. Remote sensing monitoring of *Spartina alterniflora* in coastal intertidal zone of Guangxi. Guangxi Sciences, 24(5): 483–489

Tian Yanlin, Jia Mingming, Wang Zongming, et al. 2020. Monitoring invasion process of *Spartina alterniflora* by seasonal Sentinel-2 imagery and an object-based random forest classification. Remote Sensing, 12(9): 1383, doi: 10.3390/rs12091383

Tucker C J. 1979. Red and photographic infrared linear combinations for monitoring vegetation. Remote Sensing of Environment, 8(2): 127–150, doi: 10.1016/0034-4257(79)90013-0

Wang Qing, An Shuqing, Ma Zhijun, et al. 2006. Invasive *Spartina alterniflora*: biology, ecology and management. Acta Phytotaxonomica Sinica, 44(5): 559–588, doi: 10.1360/aps06044

Yao Hongyan, Liu Pudong, Shi Runhe, et al. 2017. Extracting the transitional zone of *Spartina alterniflora* and *Phragmites australis* in the wetland using high-resolution remotely sensed images. Journal of Geo-information Science, 19(10): 1375–1381

Zhu Yuling, Wang Janbu, Wang Andong, et al. 2019. Remote-sensed monitoring of *Spartina alterniflora* using deep convolutional neural network method with fusion of shallow features. Marine Sciences, 43(7): 12–22

Zuo Ping, Liu Chang'an, Zhao Shuhe, et al. 2009. Distribution of *Spartina* plantations along the China's coast. Haiyang Xuebao (in Chinese), 31(5): 101–111

Zuo Ping, Zhao Shuhe, Liu Chang'an, et al. 2012. Distribution of *Spartina* spp. along China's coast. Ecological Engineering, 40: 160–166, doi: 10.1016/j.ecoleng.2011.12.014